WOOD RESEARCH
63 (3): 2018
419-430

DEGRADATION FEATURES OF ARCHAEOLOGICAL WOOD SURFACE TO DEEP INSIDE A CASE STUDY ON WOODEN BOARDS OF MARQUIS OF HAIHUN'S OUTER COFFIN

Yihang Zhou, Kai Wang, Dongbo Hu
Peking University, School of Archaeology and Museology
Beijing, China

Li Guan
Jiangxi Provincial Institute of Cultural Relics and Archaeology
Jiangxi, China

Hao Wu
Jingzhou Cultural Relics Protection Centre
Hubei, China

(Received October 2017)

ABSTRACT

Although researches have been carried on the bio-chemical deterioration of archaeological wood, still the degradation of archaeological wood is so complicated to fully understand. One essential question is how archaeological wood of large volume would degrade from surface to deep inside and why. The recently unearthed outer coffin of Marquis of Haihun, buried for over 1800 years, gave us a great opportunity to investigate this question. The degradation features were analyzed with methods of optical microscopy, Fourier Transform Infrared Spectroscopy (FT-IR), X-ray diffraction (XRD), viscosimetry, and determination of physical properties of wood. The results, including the microstructures of wood fibers, wood components, degree of polymerization and crystallinity of cellulose, and shrinkage of wood, unanimously show that the sapwood of the board is worst degraded, the surface layer of the heartwood is degraded to a higher extent than the inner part, and it tends to degrade more easily along the axial direction.

KEYWORDS: Archaeological wood, outer coffin, wood degradation, Marquis of Haihun.

INTRODUCTION

Archaeological wooden objects are inevitable to degrade over hundreds of years of burial underground while their degradation process are quite different from wood decays on surface environments. Both wood scientists and conservators of wooden relics show great curiosities and attentions in deterioration of archaeological wood. Microbial decay by fungi or bacteria in archaeological wood is often one of the major causes of wood degradation and the degradation features vary from one microbial species to another (Björdal et al. 1999, Nelson et al. 1995, Kim et al. 1996). We can also preliminarily understand the structure and degradation process for waterlogged wood by microscopy (Hoffman, et al. 1990). Chemical analysis, such as FT-IR, GC-MS, NMR and GPC, is an effective and essential way to characterize the degradation features (Pandey and Ptiman 2003, Łucejko et al. 2009, Colombini et al. 2009). However, it remains an essential question how archaeological wood would degrade from surface to deep inside after thousands of years' burial underground? Thanks to the recent excavation of Marquis of Haihun's tomb, we had the precious opportunity to investigate the wooden outer coffin before the archaeological wood exposed in atmosphere surroundings excessively or preservation measures were implement.

First discovered in March 23 in 2011, the tomb of Liu He, commonly known as Marquis of Haihun, also a deposed emperor of the Western Han Dynasty, has been one of the hottest archaeological excavations in China these years. It is located on the Guodun Hill in Datangping Township, Nanchang City, Jiangxi Province, which is so far the largest and best-preserved tomb of Western Han Dynasty with an abundance of buried objects found in southern China (Yang 2016). The outer coffin of Marquis of Haihun is approximately 10 meters wide and 2 meters in height, consisting of a number of wooden boards. Each board was manufactured from a fully-grown *Phoebe zhennan* tree.

By analyzing the degradation features of Marquis of Haihun's outer coffin from different depth of different anatomical directions, it is possible for us to better understand how archaeology wood of large volume would decay in the burial environment.

MATERIALS AND METHODS

Samples

In order to fully understand the degradation features of the whole wooden board, from the inner part to the surface, we used an increment borer (5.15 mm) by Haglöf Sweden® to extract a number of slender cylindrical samples in both axial and radial directions (Figs. 1 and 2). These samples were divided into appropriate subsections standing for different depths of the board for the following tests. The samples, once taken from the wooden board, were immediately put into PMMA tubes sealed with rubber caps to prevent from further dehydration. Apart from the heartwood samples extracted by an increment borer, there were also sapwood samples taken from the undersides of the boards that made up the bottom of the outer coffin. The wood species is identified as *Lauraceae Phoebe zhennan*. Sound wood of the same species is prepared and analyzed when comparison is necessary.

Fig. 1: Wooden board after extraction of samples in axial direction.

Fig. 2: Wooden board after extraction of samples in radial direction.

Microscopy

Paraffin sections were prepared as per the standard procedures and the degradation in microstructure and birefringence observed under the polarizing microscope (Leica DM4500P). Also, periodic acid -Schiff (PAS) stain and toluidine blue (TB) stain were applied to help determine the relative contents of cellulose and lignin in cell walls.

Transform Infrared Spectroscopy(FT-IR)

FT-IR was applied to test the relative quantities of functional groups and indicate the variation of contents of cellulose, hemicellulose and lignin after degradation. The wooden board samples were smashed into granules over 60 mesh and tested by FT-IR (Thermo Fisher Nicolet IS50), with a range from 4000 cm^{-1} to 400 cm^{-1}.

X-ray diffraction (XRD)

The cellulose crystallinity was tested by XRD method to examine how cellulose crystallinity may change. The samples were smashed into granules over 60 mesh, tableted and tested by Rigaku Dmax/2400 X-ray powder diffraction with Cu $K_{\alpha 1}$ radiation. The working voltage of X-ray tube was 40 kV and electric current 100 mA. The scanning coverage is from 3° to 40° with a speed of $6°{\cdot}min^{-1}$. We applied Segal method (Segal 1959), based on the intensity measured at two points in the diffractogram, to calculate the crystallinity: $X_C=(I_{200}-I_{am}) / I_{200} \cdot I_{200}$ represents both crystalline and amorphous materials while I_{am} represents amorphous material only.

Viscosimetry

The degree of polymerization (DP) is an important property to polymer like cellulose, which can be determined by the viscosimetry method (Manat 2006).

Cellulose preparation: first, the acid detergent fiber (ADF) was prepared by detergent method (Soest 1963, Soest and Vine 1967) from the original wood samples. Then, the ADF was heated in 1% chlorous acid (sodium chlorite with acetic acid) at 75°C until the fiber turned into white color. The fiber was washed in distilled water and acetone for 3 times and dried at 110°C.

Determination: An appropriate amount of cellulose fiber was weighted and dissolved in 0.5 $mol{\cdot}L^{-1}$ cuene (CED). The flow time of CED solution and cellulose-CED solution of the fixed concentration were measured by a capillary viscometer. The intrinsic viscosity was calculated according to Martin formula and the polymerization degree calculated according to Mark equations: $[\eta] = K\ M_\eta^\alpha$ (Burkus 2003). Parameter K is $2.8{\times}10^{-4}$ g/(100 mL) and α is 0.8 for cellulose-CED solution at 25°C (Yang 2001).

Determination of physical properties

The moisture contents, basic density and shrinkage of the wood samples were determined with reference to ISO standard 'Physical and mechanical properties of wood -- Test methods for small clear wood specimens – part 1, 2, 13 &14' (ISO 13061-1:2014, ISO 13061-2:2014, ISO 13061-13:2016 and ISO 13061-14:2016).

RESULTS AND DISCUSSION

Microstructure and birefringence

Under the microscope, the extent of degradation varies from the inner part of the wooden board to the surface, especially in axial direction. The surface sample in axial direction (Figs. 3 and 4) shows that almost all of the fibers have completely lost their original cell structure and birefringence and become dark brown, while most of the vessels, paratracheal parenchyma and rays still possess obvious but weak birefringence. Thus, in the heartwood samples, all kinds of parenchyma are less degradable than fibers. As the depth increases, the extent of degradation gets much better in both microstructure and birefringence (Figs. 5 and 6). However, no changes in cell structure are observed in the samples of radial direction (Fig. 7). The birefringence of fibers has become weakened but not vanished (Fig. 8), which gets more obvious as the depth increases.

The sapwood sample (Fig. 9) has decayed more severely than any of the heartwood samples, which macroscopically presents itself with severe cracks, distortion and alteration in color. Almost all the cells of both fibers and parenchyma lost its microstructure and birefringence.

After being stained with PAS-TB, the middle lamella (ML), corners (C) and secondary walls (S_1~S_3) can be easily distinguished (primary walls are too thin). For normal wood fibers stained with PAS-TB, ML and S_2 are purple while S_1 and S_3 are blue as a result of the relative contents of lignin, holocellulose and pectin. But for the severely decayed samples such as the sapwood sample and the surface sample in axial direction (Fig. 10), the whole secondary walls of the fiber cells are blue while the ML and C remain purple, which indicates a distinct cellulose loss in secondary walls, specifically in S_2. In comparison, the cellulose and pectin in ML seems to be much stable. There are also some tiny purple dots within fibers, which turn out to be hypha when observed in radial section (Fig. 11). With reference to the characteristics of decay, the hypha should belong to brown rot fungi (Schwarze 2007).

Since fibers and vessels array in axial direction, their lumens make it easier for microbial invasion and matter transmission. Nevertheless, in radial direction, it is hard for both chemicals and microbes to pass through the cell walls, meanwhile the only tunnels-rays are mostly filled with gums which helps resist the invasion of harmful factors. In the sapwood samples where gums barely exist, the parenchyma is so easy to degrade as fibers although the secondary walls in fibers are still the main distress area.

It is noteworthy that there are lots of gelatinous fibers (G-fibers) in early wood in the 14 cm deep sample in axial direction (Fig. 12), which is the signature of tension wood. For the past several decades, the G-layer has generally been presumed to be composed nearly entirely of crystalline cellulose (Bowling and Vaughn 2008). However, the birefringence in Fig. 13 is quite weak. Also, in the DP and crystallinity results (Tab. 4), we notice that the data of the deepest sample in axial direction disobey normal variation tendency and relatively lower than expected. It seems that the unlignified G-layer is more likely to lose its DP and crystallinity.

Fig. 3: Surface sample in axial direction, heartwood.

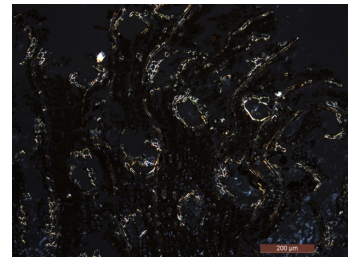

Fig. 4: Surface sample in axial direction, heartwood, under cross polarizer.

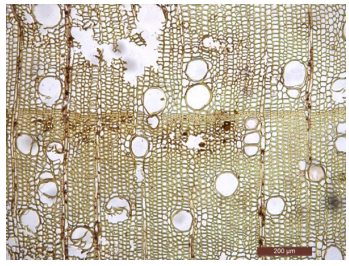

Fig. 5: 0.8 cm deep in axial direction, heartwood.

Fig. 6. 0.8 cm deep in axial direction, heartwood, under cross polarizer.

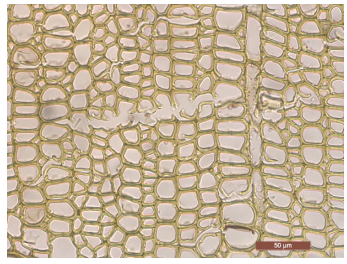

Fig. 7: Surface sample (actually 0-2mm deep) in radial direction, heartwood.

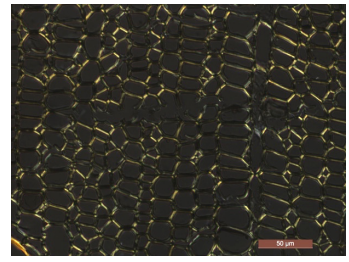

Fig. 8: Surface sample (actually 0-2mm deep) in radial direction, heartwood, under cross polarizer.

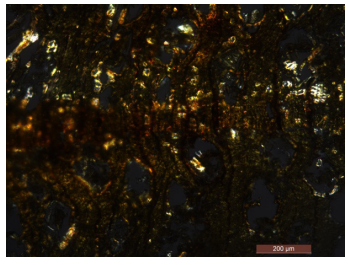

Fig. 9: Sapwood sample, under cross polarizer.

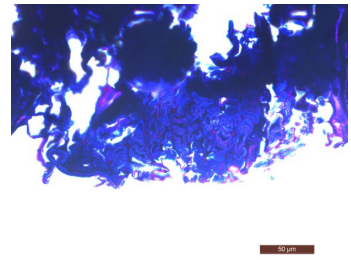

Fig. 10: Sapwood sample stained with PAS-TB.

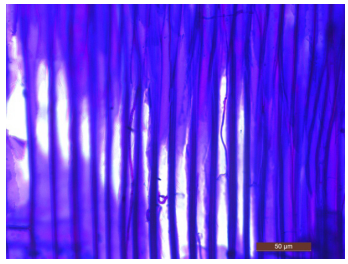

Fig. 11: Hypha in fibers.

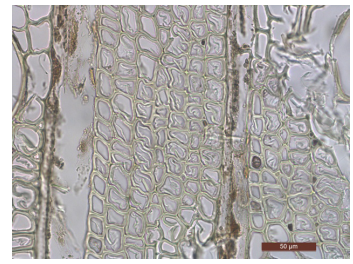

Fig. 12: Gelatinous fibers, 14cm deep in axial direction.

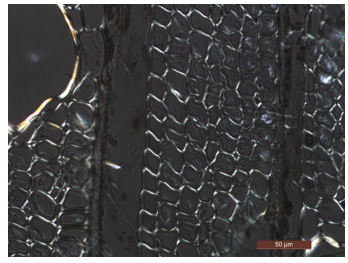

Fig. 13: Gelatinous fibers, 14cm deep in axial direction, under cross polarizer.

Components by FT-IR

The FT-IR spectrogram of sound *P. zhennan* wood is displayed in Fig. 14. The main absorption peaks of sound *P. zhennan* wood and their assignments are listed in Tab. 1. Some of the bands are quite helpful to determine the relative contents of lignin, cellulose and hemicellulose in degraded wood. In archaeological wood, the content of lignin and its structure are very close to those of the sound wood of the same species, if no microbial deterioration took place (Colombini et al. 2009). Although white rot fungi can degrade lignin, brown rot fungi can only modify lignin structure to a limited extent (Eriksson et al. 1990). Among the samples studied, only brown rot fungi prove to exist by microscopy.

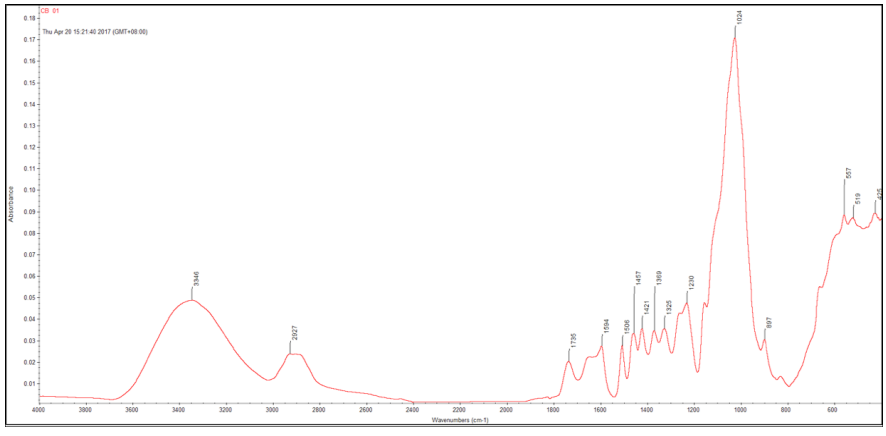

Fig. 14: FT-IR spectrogram of sound P. zhennan wood.

Also, based on the stain results, the loss of cellulose is much bigger than that of lignin. Thus, the intensity of the lignin associated band at 1506 cm^{-1} is chosen as the benchmark. The ratios of the intensity of the lignin associated bands and carbohydrate bands with I_{1506} are listed in Tab. 2 and the wavenumbers of lignin associated bands are listed in Tab. 3.

Tab. 1: FT-IR absorption peak location and assignment of P. zhennan wood (Harrington et al. 1964, Hergert 197, Schultz and Glasser 1986, Schultz 1992, Pandey and Pitman 2003).

Wavenumber/ cm^{-1}	Absorption peak assignment
3446	O-H stretching in hydroxyl groups
2927	C-H stretching
1735	Unconjugated C=O in xylans (hemicellulose)
1633	Absorbed O-H and conjugated C-O
1594	Aromatic skeletal in lignin
1506	Aromatic skeletal in lignin
1456	C-H deformation in lignin and carbohydrates
1424	Aromatic skeletal and C-H deformation
1369	C-H deformation in cellulose and hemicellulose
1325	C-H vibration in syringyl derivatives
1269	Guaiacyl ring breathing, C-O stretch in lignin and C-O linkage in guaiacyl aromatic methoxyl groups
1230	Syringyl ring and C-O stretch in lignin and xylan
1161	C-O-C vibration in cellulose and hemicellulose
1024	C-O stretch in cellulose and hemicellulose
897	C-H deformation in cellulose

I_{1735}/I_{1506} mainly represents the relative content of hemicellulose. Compared with the control (0.727), the sapwood sample (0.068) has almost lost all its hemicellulose. The ratios of I_{1735}/I_{1506} of the heartwood samples are from 0.189 to 0.306, also indicating remarkable losses in hemicellulose. Moreover, heartwood samples in axial direction possess a lower I_{1735}/I_{1506} value (0.189 - 0.265) than those in radial direction (0.227 - 0.306), which means the hemicellulose of the wooden board along the axial direction tends to degrade more easily. I_{897}/I_{1506} represents the relative content of cellulose. The ratio of the sapwood sample (0.20) indicates a remarkable drop in the relative content of cellulose. With the gradual increase of depth, the ratios of heartwood samples in both axial and radial directions ascend (except the last ones probably associated with tension wood or juvenile wood), indicating the increases in the contents of cellulose. The values of I_{1329}/I_{1506} of the heartwood samples are from 1.02 to1.10, a slight drop from 1.25 (sound wood) while the sapwood sample's ratio is 0.438 that also shows a great loss of holocellulose in the sapwood.

Although the contents of lignin of the samples are unlikely to decrease remarkably, chemical changes are still inevitably taking place all the time. One of the most common chemical modifications is demethylation of both guaiacyl and syringyl lignin units (Łucejko et al. 2009, Colombini et al. 2009). After demethylation, oxidation will then probably happen in phenol units. This chemical process causes a decrease in the quantity of ether bonds, which can be inferred by the reduced I1261/I1506 and I1230/I1506 ratios and wavenumber shifts of P_{1261} and P_{1230} of both heartwood and sapwood samples. Furthermore, the ratios of I_{1261}/I_{1506} and I_{1230}/I_{1506} go up with the increase of depth in both axial and radial directions, indicating the different levels of demethylation and oxidation from the inner part to the surface of the wooden board.

An interesting phenomenon is that an unusual drop was detected in the content, crystallinity and degree of polymerization (as detailed in the following section) of cellulose in the sample from the deepest inside in radial direction. Since the inner part of the board should be a better-preserved one presumably, attentions should be paid to prevent from wrong conclusion. I_{1594}/I_{1506} ratios can determine the relative content of syringyl lignin units: the more syringyl units, the higher the ratios will be (Faix and Beinhoff 1988, Oven and Thomas 1989). Also, it was observed that the wavenumbers of the maxima move continuously from 1510 cm^{-1} to 1504 cm^{-1} when the S content in GS lignin increases (Faix and Beinhoff 1988). According to both I_{1594}/I_{1506} ratios and the wavenumbers of the maxima, the sample from the deepest inside in radial direction is confirmed as juvenile wood due to the lower content of syringyl units. Moreover, outer heartwood was found to be more resistant to than inner heartwood (possibly juvenile wood) when exposed to the brown rot fungus Poria placenta according to the literature (Flæte 2004). It likely that the juvenile wood may degrade more easily. Thus, the low content, crystallinity and DP of the cellulose in the deepest sample are probably inherent and reasonable.

Tab. 2: Ratios of the intensity of the lignin associated bands and carbohydrate bands with I_{1506}.

Sample (depth from the surface)		I_{1735}/I_{1506}	I_{1594}/I_{1506}	I_{1369}/I_{1506}	I_{1261}/I_{1506}	I_{1230}/I_{1506}	I_{897}/I_{1506}
Sound *P. zhennan* wood (control)		0.727	0.985	1.25	1.55	1.72	1.10
Sapwood sample		0.068	0.838	0.438	0.990	1.20	0.20
Heartwood in radial direction	0-2cm	0.306	1.00	1.02	1.20	1.15	0.827
	2-4cm	0.277	1.00	1.04	1.25	1.19	0.831
	4-6cm	0.227	0.962	1.03	1.24	1.17	0.951
	6-8cm	0.242	0.942	1.04	1.30	1.20	0.867
Heartwood in axial direction	2.5-5.5cm	0.189	1.03	1.03	1.22	1.15	0.830
	6.5-9.5cm	0.265	0.967	1.04	1.23	1.15	0.872
	10.5-13.5cm	0.245	0.995	1.05	1.27	1.23	1.08
	14.5-17.5cm	0.257	0.997	1.10	1.32	1.25	0.997

Tab. 3: Wavenumbers of part of lignin associated bands.

Sample (depth from the surface)		P_{1594}/cm^{-1}	P_{1506}/cm^{-1}	P_{1325}/cm^{-1}	P_{1261}/cm^{-1}	P_{1230}/cm^{-1}
Sound *P. zhennan* wood		1594	1506	1325	1261	1230
Sapwood sample		1592	1504	1326	1264	1220
Heartwood in radial direction	0-2cm	1594	1506	1326	1265	1227
	2-4cm	1594	1506	1323	1265	1227
	4-6cm	1593	1506	1324	1265	1227
	6-8cm	1594	1507	1323	1265	1228
Heartwood in axial direction	2.5-5.5cm	1594	1506	1326	1265	1227
	6.5-9.5cm	1594	1506	1326	1265	1227
	10.5-13.5cm	1593	1506	1324	1265	1227
	14.5-17.5cm	1594	1506	1326	1265	1228

Crystallinity and DP of cellulose

The crystallinity and degree of polymerization (DP) are both important parameters for wooden objects, influencing their Young's modulus and dimensional stability. Both sapwood and heartwood show an evident drop in crystallinity. The crystallinity and DP of heartwood samples in both radial and axial directions increase as the depth increases (Tab. 4). This variation tendency of degradation is synchronous with the other degradation features discussed above. However, the main causes of the loss in crystallinity and DP are quite different.

Tab. 4: Crystallinity and DP of cellulose in the wooden board.

Sample (depth from the surface)		DP (×102)	Crystallinity (%)
Sound *P. zhennan* wood		6.1	75.3
Sapwood sample		/	38.7
Heartwood in radial direction	0-2cm	4.8	40.7
	2-4cm	5.7	46.7
	4-6cm	6.2	51.5
	6-8cm[a]	4.1	45.3
Heartwood in axial direction	0-2.5cm	4.8	/
	2.5-5.5cm	5.8	41.6
	6.5-9.5cm	6.1	56.8
	10.5-13.5cm	6.8	64.8
	14.5-17.5cm[b]	5.4	58.5

[a] This sample is juvenile wood with originally low crystallinity and DP, which is discussed in FT-IR part and excluded in this discussion; b this sample shows a decrease in crystallinity and DP, which is probably caused by the gelatinous fibers observed and discussed in the microstructure part and thus excluded.

The acidic red soil in the burial environment and the acidity of wood itself provide advantageous condition for cellulose hydrolysis. Another important factor is the oxidation of cellulose, possibly an alternative cause in depolymerization. But it can be expected that the oxidation proceeds first on lignin, which functions chemically as an antioxidant in plants according to the literature (Ponomarenko et al. 2015). In relatively sealed conditions in the tomb underground, the oxidation of cellulose can be inferred to be very limited, which is also supported by I1735/I1506 ratios in FT-IR results. Nevertheless, we may infer that the oxidation of both lignin and even holocellulose as well results in a combination of different carbonyl groups of different oxidation states which increase the acidity and thus promote the hydrolysis process eventually. Moreover, the consumption of oxygen creates an oxidation potential gradient from the surface to deep inside and the acidity gradient consequently which explain the tendency of cellulose degradation.

Although the hydrolysis of cellulose alone usually leads to an increase in crystallinity since chemical reactions tend to happen in the amorphous region of cellulose, yet it is not the only factor. Buried in a water-saturated condition for thousands of years, hydrone and ions continuously broke original hydrogen bonds in both amorphous and crystalline regions of cellulose, resulting in a decrease in crystallinity.

Determination of physical properties

Like the degradation features in micro and chemical aspects, the macro features also vary from the deep inside to the surface (Tab. 5). But not all the physical properties are proper to

assess the degradation. The basic density and moisture contents don't show the tendency as they should be. Since the wooden boards of the outer coffin were partly dehydrated during and after the excavation, consequently, the basic density became higher and the moisture contents became lower, especially the part close to the surface.

Tab. 5: Physical properties of the wooden board.

Sample (depth from the surface)		Basic density ($g \cdot cm^{-3}$)	Moisture content (%)	Linear shrinkage (%)[a]	Body shrinkage (%)
Heartwood in axial direction	2-5.5cm	0.495	126.9	0.5	42.7
	6.5-9.5cm	0.483	138.4	1.0	39.4
	10.5-13.5cm	0.508	131.3	0.3	34.8
	14.5-17.5cm	0.495	147.9	0.3	33.0
Heartwood in radial direction	0-2cm	0.482	144.7	20.0	49.1
	2-4cm	0.453	157.0	19.0	49.2
	4-6cm	0.451	165.1	17.3	47.4
	6-8cm	0.458	162.1	15.5	42.4
Sound *P. zhennan* wood		0.497	124.0	/	5.3

[a] The direction of linear shrinkage is the same as the sampling direction because the samples extracted by an increment borer are slender cylindrical.

Also, it is faster to dehydrate in axial direction according to the data. The linear shrinkages of the samples in axial direction are almost the same as sound wood while those in radial direction increase markedly with the gradual decrease of depth, which indicates the radial intensity and the size stability are more likely to descend. On the basis of the data in Tab. 5, body shrinkage seems to be the best parameter to determine the degree of degradation if radial linear shrinkage is unable to test.

CONCLUSIONS

It is effective to analyze the degradation features by using microscopy, FT-IR, XRD, viscosimetry and determination of physical properties. There is a similar variation tendency in microstructure, wood components, DP, crystallinity and shrinkage from surface to deep inside of the wooden board. The results from various aspects show that the sapwood of the board is worst degraded, the surface layer of the heartwood is degraded to a higher extent than the inner part of the board, and it tends to degrade more easily along the axial direction. The fillers like gums in parenchyma of heartwood, the anatomical structure of *P. zhennan* wood and the conditions such as oxidation potential and acidity varying from the deep inside to the surface may explain the degradation differences.

REFERENCES

1. Björdal, C.G., Nilsson, T., Daniel, G., 1999): Microbial decay of waterlogged archaeological wood found in Sweden applicable to archaeology and conservation, International Biodeterioration & Biodegradation 43(1–2): 63-73.

2. Burkus, Z., Temelli, F., 2003: Determination of the molecular weight of barley β-glucan using intrinsic viscosity measurements, Carbohydrate Polymers 54(1): 51-57.
3. Bowling, A. J., Vaughn, K. C., 2008: Immunocytochemical characterization of tension wood: gelatinous fibers contain more than just cellulose, American Journal of Botany 95(6): 655-63.
4. Colombini, M. P., Lucejko, J. J., Modugno, F., Orlandi, M., Tolppa, E. L., Zoia, L., 2009: A multi-analytical study of degradation of lignin in archaeological waterlogged wood, Talanta 80(1): 61-70.
5. Eriksson, K. E. L., Blanchette, R. A., Ander, P., 1990: Microbial and enzymatic degradation of wood and wood components. Microbial and enzymatic degradation of wood and wood components. Springer Berlin, Heidelberg, 333 pp.
6. Faix, O., Beinhoff, O., 1988: FTIR spectra of milled wood lignins and lignin polymer models (dhp's) with enhanced resolution obtained by deconvolution, Journal of Wood Chemistry & Technology 8(4): 505-522.
7. Flæte, P. O., 2004: Non-destructive prediction of decay resistance of heartwood by near infrared spectroscopy, Scandinavian Journal of Forest Research 19(5): 55-63.
8. Hoffmann, P., Jones, M. A., Rowell, R. M., Barbour, R. J., 1990: Structure and degradation process for waterlogged archaeological wood, Archaeological Wood: Properties, Chemistry, and Preservation 1: .35-65).
9. Harrington, K. J., Higgins, H. G., Michell, A. J., 1964: Infrared spectra of *Eucalyptus regnans* F. Muell. and *Pinus radiata* D. Don, Holzforschung 18(4): 108-113.
10. Kim, Y. S., Singh, A. P., Nilsson, T., 1996: Bacteria as important degraders in waterlogged archaeological woods, Holzforschung 50(5): 389-392.
11. Łucejko JJ, Modugno, F., Ribechini, E. del Río, J. C., 2009: Characterisation of archaeological waterlogged wood by pyrolytic and mass spectrometric techniques, Analytica Chimica Acta 654(1): 26-34.
12. Manat, H., Nurmmamat, 2006: Determination of polymerization degree of plant cellulose by viscosimetry, China Synthetic Fiber Industry 29(1): 40-42.
13. Nelson, B. C., Goñi, M. A., Hedges, J. I., Blanchette, R. A., 1995: Soft-rot fungal degradation of lignin in 2700-year-old archaeological woods, Holzforschung 49(1): 1-10.
14. Owen, N.L., Thomas, D.W., 1989: Infrared studies of "Hard" and "Soft" woods, Applied Spectroscopy 43: 451–455.
15. Ponomarenko, J., Lauberts, M., Dizhbite, T., Lauberte, L., Jurkjane, V., Telysheva, G., 2015: Antioxidant activity of various lignins and, lignin-related phenylpropanoid units with high and low molecular weight, Holzforschung 69(6): 795-805.
16. Pandey K K, Pitman A J., 2003: FTIR studies of the changes in wood chemistry following decay by brown-rot and white-rot fungi, International Biodeterioration & Biodegradation 52(3):151-160.
17. Segal, L. C., Creely, J., Martin, A. E. J., Conrad, C. M., 1959: An empirical method for estimating the degree of crystallinity of native cellulose using the x-ray diffractometer, Textile Research Journal 29(10): 786-794.
18. Soest, V., P., J., 1963: Use of detergents in the analysis of fibrous feeds. 2. a rapid method for the determination of fiber and lignin, Journal - Association of Official Analytical Chemists, 49: 546-551.
19. Soest, P. J. V. Vine, R.H., 1967: Use of detergents in the analyses of fibrous feeds. part IV. determination of plant cell wall constituents, Journal - Association of Official Analytical Chemists 50: 50-55.

20. Schwarze, F. W. M. R., 2007: Wood decay under the microscope, Fungal Biology Reviews 21(4): 133-170.
21. Schultz, T. P., Glasser, W. G., 1986: Quantitative structural analysis of lignin by diffuse reflectance Fourier transform spectrometry, Holzforschung 40: 37-44.
22. Schultz, T. P., 1992: Infrared study of lignin: reexamination of aryl-alkyl ether C-O stretching peak assignments, Holzforschung 46(6): 523-528.
23. Yang, S.H., 2009: Plant fiber chemistry (Third edition), Beijing: China Light Industry Press, (in Chinese).
24. Yang, J., Xu, C. Q., 2016: Marquis of Haihun's tomb of Western Han in Nanchang, Archaeology (7): 45-62 (in Chinese).

Yihang Zhou, Kai Wang, Dongbo Hu*
Peking University
School of Archaeology and Museology
Beijing
China
Corresponding author: 18811723499@126.com

Li Guan
Jiangxi Provincial Institute of Cultural Relics and Archaeology
Jiangxi
China

Hao Wu
Jingzhou Cultural Relics Protection Centre
Hubei
China